

Niobium- and Tantalum-Based Ethylene Polymerisation Catalysts Bearing Methylene- or Dimethyleneoxa-Bridged Calixarene Ligands

Carl Redshaw,^{*[a]} Michael Rowan,^[a] Damien M. Homden,^[a] Mark R. J. Elsegood,^[b] Takehiko Yamato,^[c] and Carol Pérez-Casas^[c]

Abstract: Treatment of *p*-*tert*-butylcalix[6]areneH₆ (H₆*t*Bu-L) or *p*-*tert*-butylcalix[8]areneH₈ (H₈*t*Bu-L¹) with [MCl₅] (M=Nb, Ta) in refluxing toluene or dichloromethane affords, after work-up, the complexes [[M(NCMe)Cl₂]₂(*t*Bu-L)] (M=Nb (**1**), Ta (**2**)) and [(MCl₂)₂(*t*Bu-L¹H₂)] (M=Nb (**4**), Ta (**5**)), respectively. Complex **1**, as well as [[Nb₂(μ-O)₂(μ-Cl)(*t*Bu-LH)]₂] (**3**), is also available from [NbOCl₃] and H₆*t*Bu-L. Reaction of [MOCl₃] (M=Nb, Ta) with Li₃(*t*Bu-L²) in diethyl ether, where H₃*t*Bu-L² is *p*-*tert*-butylhexahomotrioxa-

calix[3]areneH₃, affords, after work-up, the trimeric complexes [[M(*t*Bu-L²)(μ-O)]₃] (M=Nb (**6**), Ta (**7**)). The behaviour of **1** to **7** (not **3**), as well as the known complexes [[(MCl)*p*-*tert*-butylcalix[4]arene]₂] (M=Nb (**8**), Ta (**9**)) and [(MCl₂)*p*-*tert*-butylcalix[4]arene(OMe)] (M=Nb (**10**), Ta (**11**)), as precatalysts for the polymerisation of ethylene has been investigated. In the

Keywords: calixarenes • ethylene • niobium • polymerization • tantalum

presence of dimethyl (or diethyl)aluminium chloride, methylaluminumoxane or trimethylaluminium, these niobium and tantalum precatalysts are all active (<35 gmmol⁻¹h⁻¹bar⁻¹), for the polymerisation of ethylene affording high-molecular-weight linear polyethylene. The dimethyleneoxa-bridged systems (derived from **6** and **7**) are more active (84 and 46 gmmol⁻¹h⁻¹bar⁻¹, respectively) than the methylene-bridged systems. The molecular structures of **1–6** and **10** (acetonitrile solvate) are reported.

Introduction

In α -olefin polymerisation, the use of macrocycles, most notably calixarenes, as ancillary ligands has, to date, had only limited success.^[1] Catalytic activities reported are at best moderate (<100 gmmol⁻¹h⁻¹bar⁻¹), the only exception is the chromium(III) calix[4]arene system of uncertain precatalyst structure reported by Kim and co-workers, which polymerises ethylene with activities as high as 1500 gmmol⁻¹h⁻¹

at 35 bar.^[2] However, recently we have found that vanadyl complexes bearing dimethyleneoxa-bridged (-CH₂OCH₂-) oxacalix[3]arenes form extremely active catalytic species upon interaction with dimethylaluminium chloride (DMAC) in the presence of the re-activator ethyl trichloroacetate (ETA). Under the same catalytic conditions, vanadyl complexes bearing methylene-bridged (-CH₂-) calix[4]arenes proved to have far inferior activities, though still far better than those observed previously for calix[4]arene-based systems.^[3] Herein, we extend these studies to the other Group 5 metals, niobium and tantalum, and report the synthesis, characterisation and ethylene polymerisation behaviour of calix[*n*]arenes (*n*=4, 6 and 8), and compare this behaviour with that of related oxacalix[3]arene complexes. Metallocalix[*n*]arenes incorporating niobium or tantalum are rather rare, with reports restricted to the calix[4]arene work of Floriani and co-workers^[4] and more recently Radius and co-workers.^[5] Indeed, the transition-metal coordination chemistry of the larger (*n*>4) calix[*n*]arenes is in general rather limited,^[6] doubtless due to problems associated with product crystallisation, characterisation and cost. Furthermore, investigations of oxacalix[3]arene transition-metal chemistry are at an embryonic stage, reflected in the mere handful of reports in the literature.^[7]

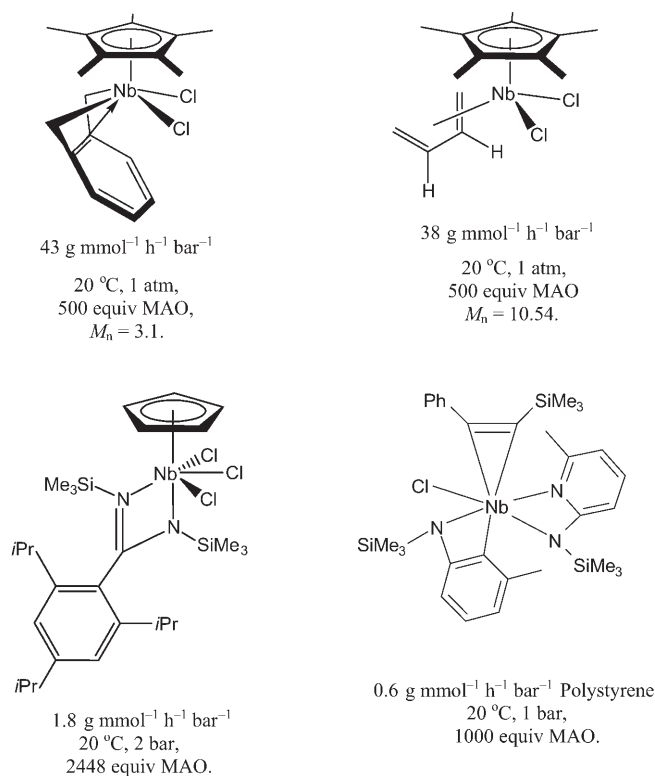
[a] Dr. C. Redshaw, Dr. M. Rowan, D. M. Homden
Wolfson Materials and Catalysis Centre
School of Chemical Sciences and Pharmacy
University of East Anglia, Norwich, NR4 7TJ (UK)
Fax: (+44) 1603-593137
E-mail: carl.redshaw@uea.ac.uk

[b] Dr. M. R. J. Elsegood
Chemistry Department, Loughborough University
Loughborough, Leicestershire, LE11 3TU (UK)

[c] Prof. T. Yamato, Dr. C. Pérez-Casas
Department of Applied Chemistry
Faculty of Science and Engineering
Saga University, Honjo-machi 1, Saga-shi, 840-8502 (Japan)

Supporting information for this article is available on the WWW under <http://www.chemistry.org> or from the author.

Niobium- and tantalum-based systems for the polymerisation of ethylene are also relatively rare, and with the exception of the aminopyridinato complexes $[\text{TaCl}_3(\text{NpyBz})_2]$ ($\text{Bz} = \text{benzyl}$) and $[\text{TaCl}_3(\text{PhNpyNHPPh})_2]$ (activity = $4780 \text{ g mmol}^{-1} \text{ h}^{-1} \text{ bar}^{-1}$), the amidinate complex $[\text{Cp}^*\{\text{MeC}(\text{NiPr})_2\}\text{TaCl}_3]$ (activity = $470 \text{ g mmol}^{-1} \text{ h}^{-1} \text{ bar}^{-1}$) and the di- and trimethyl complexes $[(\eta^5\text{-C}_5\text{Me}_4\text{H})\text{Ta}(\text{N}i\text{Bu})\text{Me}_2]$ and $[\{\text{ArN}(\text{CH}_2)_3\text{NAr}\}\text{TaMe}_3]$ ($\text{Ar} = 2,6\text{-}i\text{Pr}_2\text{C}_6\text{H}_3$), both of which have been used in ethylene/1-hexene copolymerisations, associated activities are low (see Schemes 1 and 2).^[8] We have

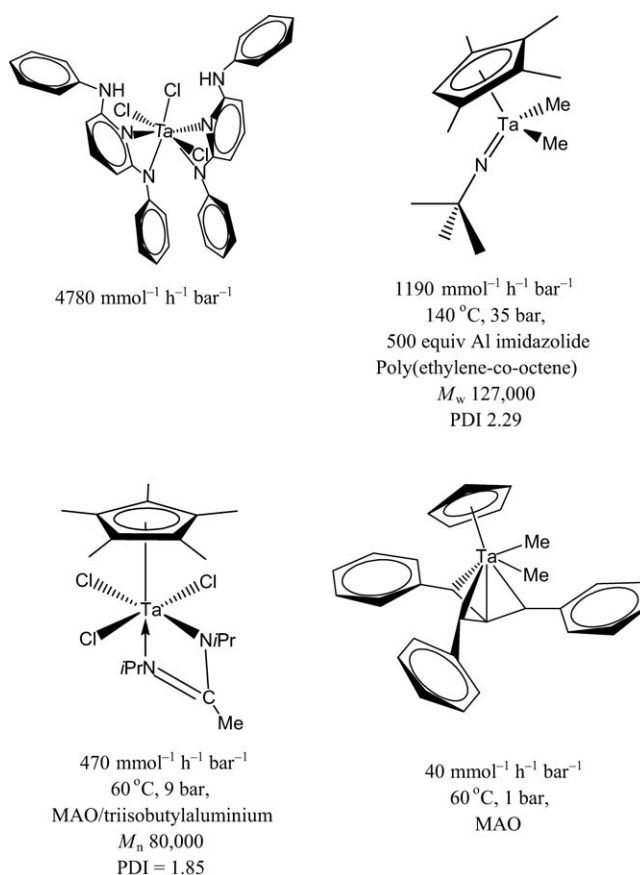


Scheme 1. Examples of niobium-based ethylene polymerisation pro-catalysts.^[11–14]

also noted low activity for systems utilising bi- and tri-dentate linear aryloxide ligation.^[9] It is also noteworthy here that there is also growing interest in the use of niobium(V) chlorides in organic synthesis.^[10]

Results and Discussion

Use of *p*-tert-butylcalix[6]arene H_6 ($H_6t\text{Bu-L}$): Reaction of H_6L with 2.2 equivalents of $[\text{NbCl}_5]$ in refluxing toluene affords, after work-up (extraction into hot acetonitrile), small orange prisms of the complex $[\{\text{Nb}(\text{NCMe})\text{Cl}_2\}_2(t\text{Bu-L})]$ (**1**) with a yield of approximately 66%. Stoichiometrically, **1** is formed by loss of three equivalents of HCl per niobium centre. In the IR spectrum of **1**, $\nu(\text{CN})$ for both coordinated ($2310/2288 \text{ cm}^{-1}$) and free acetonitrile ($2293/2251 \text{ cm}^{-1}$) are observed.



Scheme 2. Examples of tantalum-based ethylene polymerisation pro-catalysts.^[15–18]

Small crystals of the orange complex **1** suitable for single-crystal X-ray analysis by using synchrotron radiation^[19] were grown from a saturated acetonitrile solution on prolonged standing (2–3 days) at ambient temperature. The molecular structure is shown in Figure 1 and reveals the way in which the macrocyclic ring twists to accommodate the two facially coordinated niobium centres, one lying above and one below the plane of the macrocyclic ring; each niobium atom being displaced by 1.0 \AA from this plane. A consequence of the twist is the formation of two small cups, each comprising three calixarene–phenolate subunits. The geometry at each niobium centre is best described as pseudo-octahedral with *cis*-chlorines and a solvent-bound molecule. The Nb–Cl distances ($2.3805(9)$ – $2.3981(10) \text{ \AA}$) are slightly longer than those observed in $[\text{Nb}_2\text{Cl}_{10}]$ ($2.250(6)$ and $2.302(5) \text{ \AA}$)^[20] and $[\text{NbCl}(\text{mtp})_2]$ ($2.3357(9) \text{ \AA}$) ($\text{mtp} = 2,2'\text{-methylenebis}(2,4\text{-di-}i\text{-tert-butylphenol})$).^[21] The Nb–O distances (av 1.87 \AA) are typical of those in other niobium(V) aryloxides,^[22] whilst the Nb–N bonds ($\text{Nb}(1)\text{--N}(1) 2.291(2)$, $\text{Nb}(1)\text{--N}(2) 2.314(2) \text{ \AA}$) are slightly longer than those observed in $[\text{NbCl}_5(\text{NCMe})]$ ($2.236(4) \text{ \AA}$),^[23] $[\text{NbCl}_4(\text{NCMe})_2]$ ($2.220(13) \text{ \AA}$)^[24] and $[\text{Nb}\{\text{H}(t\text{BuL}^2)\}_2\text{Cl}(\text{NCMe})]$ ($2.296(5) \text{ \AA}$).^[25] There are also two acetonitrile molecules of crystallisation. One of these solvent molecules is located in one of the two cups and this is thought to account for the shielded protons at $\delta =$

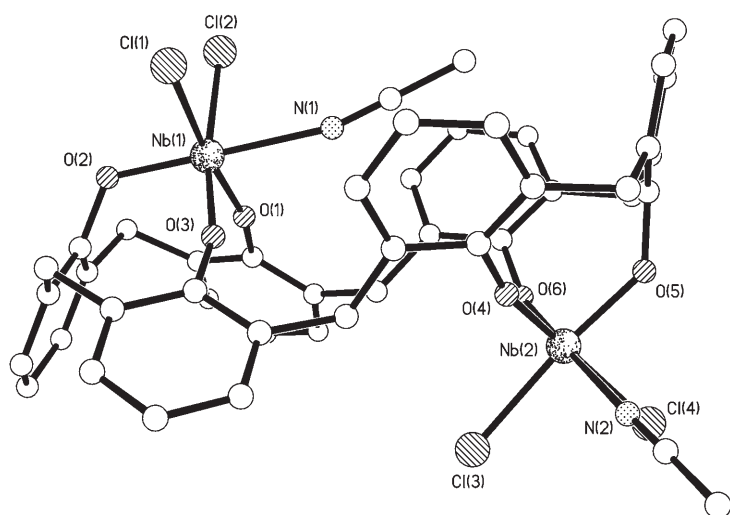


Figure 1. Molecular structure of **1**. Hydrogen atoms and calixarene *t*Bu groups omitted for clarity.

0.36 ppm in the ^1H NMR spectrum. This MeCN is disordered over two sets of positions that are approximately 90° apart with the methyl carbon atom common to both.

The reaction of $[\text{TaCl}_5]$ proceeds in much the same way as the niobium reaction outlined above, though it was found that reaction yields in the case of tantalum could be increased by exchanging the reaction solvent from toluene to dichloromethane. Reaction of $\text{H}_6\text{tBu-L}$ with 2.2 equivalents of $[\text{TaCl}_5]$ in refluxing dichloromethane affords, after work-up (extraction into hot acetonitrile), small yellow prisms of the complex $[\{\text{Ta}(\text{NCMe})\text{Cl}_2\}(\text{tBu-L})]$ (**2**) with a yield of approximately 50%. Stoichiometrically, **2** is formed by loss of three equivalents of HCl per tantalum centre. In the IR spectrum of **2**, $\nu(\text{CN})$ for both coordinated and free acetonitrile (2340 and 2295 cm^{-1} , respectively) are observed. Small crystals of the yellow complex **2** suitable for single-crystal X-ray analysis by using synchrotron radiation^[19] were grown from a saturated acetonitrile solution on prolonged standing at -10°C for one week.

The molecular structures of the calix[6]arene complexes **1** and **2** are isostructural, and selected bond lengths and angles are compared in Table 1 and illustrate the similar geometri-

Table 1. Comparison of selected bond lengths [\AA] and angles [$^\circ$] for **1** and **2**.

	1	2
M(1)–O(1)	1.871(2)	1.8742(18)
M(1)–O(2)	1.8772(19)	1.8893(17)
M(1)–O(3)	1.8748(19)	1.8786(17)
M(1)–Cl(1)	2.3981(10)	2.3994(8)
M(1)–Cl(2)	2.3805(9)	2.3809(8)
M(1)–N(1)	2.291(2)	2.232(2)
O(1)–M(1)–O(2)	92.56(8)	93.04(7)
O(1)–M(1)–O(3)	91.76(9)	91.91(8)
M(1)–O(1)–C(1)	165.82(17)	164.95(15)
M(1)–O(2)–C(12)	125.27(15)	124.47(14)
M(1)–O(3)–C(23)	162.52(17)	163.47(15)
Cl(1)–M(1)–Cl(2)	87.71(5)	87.57(4)

cal parameters of the two structures. The molecular structure of **2** is shown in Figure 2 this time viewed approximately perpendicularly to the O_6 plane; each tantalum being displaced by 1.0 \AA from this plane.

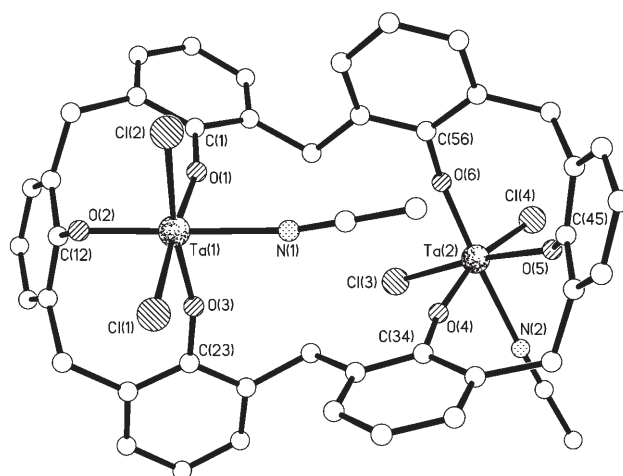


Figure 2. Molecular structure of **2**. Hydrogen atoms and calixarene *t*Bu groups omitted for clarity.

The niobium and tantalum structures are essentially identical. The Ta–Cl distances ($2.3809(8)$ and $2.3994(8)\text{ \AA}$) are similar to those observed in the anion of $[(\eta^5\text{-C}_9\text{H}_7)_2\text{TaCl}_2]\text{-}[\text{TaCl}_6]$ ($2.315(4)$ and $2.390(4)\text{ \AA}$).^[26] The Ta–O distances (av 1.88 \AA) are comparable to those of other tantalum(V) calixarenes,^[4] whilst the Ta–N bonds (Ta–N $2.232(2)$ – $2.294(2)\text{ \AA}$) are close to the range observed (2.237 – 2.367 \AA) for the nine examples in the Cambridge Structure Database.^[27] The disordered solvent molecule held within the cup is responsible for the shielded proton at $\delta = -0.36$ ppm in the ^1H NMR spectrum.

For both **1** and **2**, it is noteworthy that the ^1H NMR signals are broad in appearance at room temperature (298 K), but sharpen up on cooling to 273 K (see Supporting Information, section a, ii), consistent with a slowing down of the exchange in the CH_2 groups. At this temperature, by using homonuclear two-dimensional (2D) *J*-resolved and DFCOSY experiments, we were able to more fully assign the ArCH_2Ar resonances (see Supporting Information, section a, iii/iv). For **1**, the multiplet at about $\delta = 4.25$ ppm is thus best described as two doublets with an underlying singlet, the remaining *exo* protons appear as two doublets at around $\delta = 3.46$ ppm (each 2H with $J = 13.2$ Hz), whilst the remaining *endo* protons appear between $\delta = 5.05$ and 4.80 ppm as four doublets (each 1H with $J = 12.6$ or 13.8 Hz). Similarly for **2**, the multiplet at around $\delta = 4.28$ ppm comprises two doublets with an underlying singlet, the remaining *exo* protons appear as three doublets between $\delta = 3.46$ – 3.52 ppm (ratio 2:1:1), whilst the remaining *endo* protons appear between $\delta = 5.02$ and 4.77 ppm as four doublets (each 1H with $J = 12.6, 13.2$ or 13.8 Hz). Increasing the temperature of the samples (323 K) led to a broadening of signals (see Support-

ing Information, section a, ii) and a coalescing of those associated with the ArCH_2Ar groups, consistent with an increased rate of exchange. In the ^{13}C NMR spectrum of **1** and **2**, three ArCH_2Ar resonance signals were found between $\delta = 32.61$ and 34.41 , however, an increased number of signals assignable to both the aryl carbons (32 including 5 C_i) and the *tert*-butyl groups (four methyl and five quaternary C) were observable for **2** compared with **1** (18 including three C_i , and three methyl and one quaternary C , respectively).

Complex **1** is also available in moderate yield from the reaction of $\text{H}_6t\text{Bu-L}$ and $[\text{NbOCl}_3]$ in refluxing toluene. However, upon work-up, this reaction also affords a second paler complex with a somewhat lower yield (ca. 15%). The IR spectrum of this complex contained strong bands in the $600\text{--}800\text{ cm}^{-1}$ region consistent with $\nu(\text{Nb}\text{--}\text{O}\text{--}\text{Nb})$ vibrations of bridging oxo groups and a shoulder at 3150 cm^{-1} that suggested the presence of $\nu(\text{O}\text{--}\text{H})$. An X-ray study of the crystals obtained from a saturated solution in acetonitrile at 0°C shows the compound to be the acetonitrile solvate $[\{\text{Nb}_2(\mu\text{--}\text{O})_2(\mu\text{--}\text{Cl})(t\text{Bu-LH})_2\}]_2 \cdot 16\text{MeCN}$ (**3**). Stoichiometrically, **3** is formed through the loss of ten molecules of HCl from four equivalents of $[\text{NbOCl}_3]$. The molecular structure is shown in Figure 3; selected bond lengths and angles are given in

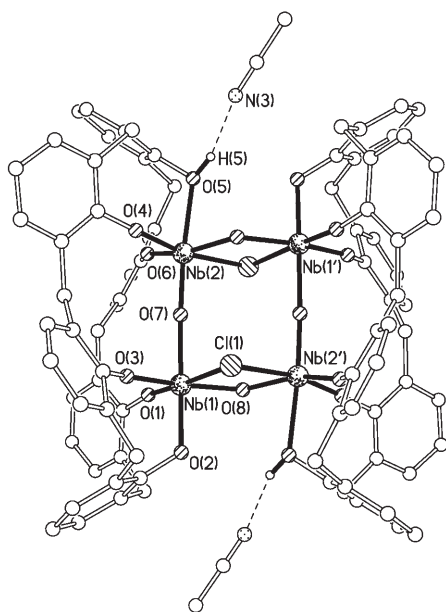


Figure 3. Molecular structure of **3**. Hydrogen atoms and calixarene *t*Bu groups omitted for clarity. Selected bond lengths [\AA] and angles [$^\circ$]: $\text{Nb}(1)\text{--}\text{O}(1)$ 1.863(3), $\text{Nb}(1)\text{--}\text{O}(2)$ 1.954(3), $\text{Nb}(1)\text{--}\text{O}(3)$ 1.931(3), $\text{Nb}(1)\text{--}\text{O}(7)$ 2.021(2), $\text{Nb}(1)\text{--}\text{O}(8)$ 1.901(3), $\text{Nb}(1)\text{--}\text{Cl}(1)$ 2.5871(13), $\text{O}(2)\text{--}\text{Nb}(1)\text{--}\text{O}(7)$ $174.54(11)$, $\text{Nb}(1)\text{--}\text{O}(7)\text{--}\text{Nb}(2)$ $177.26(15)$, $\text{Nb}(1)\text{--}\text{O}(8)\text{--}\text{Nb}(2')$ $122.10(15)$, $\text{Nb}(1)\text{--}\text{Cl}(1)\text{--}\text{Nb}(2')$ $80.80(4)$. ' atoms generated by using the symmetry operation $-x, -y+2, -z+1$.

the caption. The molecule lies on an inversion centre and consists of two *t*Bu-LH ligands each coordinated by two pseudo-octahedral niobium centres which share a linear ($177.26(15)^\circ$), asymmetric ($\text{Nb}(1)\text{--}\text{O}(7)$ $2.021(2)$, $\text{Nb}(2)\text{--}\text{O}(7)$ $1.807(2)$) $\text{Nb}\text{--}\text{O}\text{--}\text{Nb}$ bond. The two halves of the mol-

ecule are linked by a pair of μ^2 -oxo ($\text{Nb}(1)\text{--}\text{O}(8)$ $1.901(3)$, $\text{Nb}(1)\text{--}\text{O}(8)\text{--}\text{Nb}(2')$ $122.10(15)^\circ$) and chloro ($\text{Nb}(1)\text{--}\text{Cl}(1)$ $2.5871(13)$, $\text{Nb}(1)\text{--}\text{Cl}(1)\text{--}\text{Nb}(2')$ $80.80(4)^\circ$) ligands bridging $\text{Nb}(1)$ with $\text{Nb}(2')$ and $\text{Nb}(2)$ with $\text{Nb}(1)$. Alternatively, **3** may be viewed as being built up from two edge-shared bi-octahedral fragments in which each niobium centre (the niobium–niobium distance $\text{Nb}(1)\cdots\text{Nb}(2')$ is $3.3407(5)\text{ \AA}$) is coordinated in a *fac* manner by a calixarene ligand, the two fragments being linked by linear oxo bridges $\text{O}(7)$, which is a situation reminiscent of that found in the structure of $[\text{NbOCl}_3]$.^[28] The conformation of the macrocycle is best described as a slightly twisted enlarged cup. The calix[6]arene ligands lie face-to-face (intermolecular), but are slightly offset. The cavity between them contains four well-defined MeCN molecules (two unique). There are also two other larger void spaces, in which reside about ten diffuse/disordered MeCN molecules.

The remaining unique MeCN of crystallisation hydrogen bonds to $\text{O}(5)\cdots\text{H}(3)$, which has a long $\text{Nb}(2)\text{--}\text{O}(5)$ ($2.277(3)\text{ \AA}$) bond, consistent with protonation (the hydrogen atom was located from difference maps); there are thus 16 MeCN of crystallisation overall (eight unique).

Use of *p*-tert-butylcalix[8]arene H_8 ($\text{H}_8t\text{Bu-L}^1$): Interaction of $[\text{NbCl}_5]$ with 0.5 equivalents of *p*-tert-butylcalix[8]arene H_8 ($\text{H}_8t\text{Bu-L}^1$) in refluxing toluene afforded, after work-up, orange prisms of $[(\text{NbCl}_2)_2(t\text{Bu-L}^1\text{H}_2)]$ (**4**) in good yield (ca. 50–55%). As for **1**, **4** is formed stoichiometrically by loss of three equivalents of HCl per niobium centre. In the IR of this compound, a broad feature at 3158 cm^{-1} is assigned to $\nu(\text{O}\text{--}\text{H})$. The ^1H NMR spectrum (600 MHz) is consistent with the solid-state structure: the *endo*-methylene protons appear as four doublets between $\delta = 5.57\text{--}4.62$ ppm (each integrating to 2H with J between 14.0 and 17.5 Hz), whilst the *exo*-methylene protons appear as two doublets at $\delta = 3.49$ and 3.52 ppm (2H each with $J = 14.0$ and 14.5 Hz) together with a singlet at $\delta = 3.10$ ppm (4H); a singlet (integrating to 2H) appears at $\delta_{\text{OH}} = 9.79$ ppm.

Crystals of **4**·6.75 MeCN suitable for an X-ray diffraction study were grown from a hot, saturated solution of **4** in acetonitrile, on slow cooling to ambient temperature. There are two, apparently closely related, polymorphs, one in space group Pn , the other in $P2_1$. The $P2_1$ polymorph was not refined to completion due to the large structure size and problems with disorder. In both cases there are four molecules of the complex and about 27 molecules of solvent in the asymmetric unit. The calix[8]arene ring twists (see Figure 4) considerably to accommodate the two *cis*- Cl_2Nb fragments, the latter existing in local distorted octahedral environments. There is no incorporation of metal-bound solvent presumably because each niobium has already attained the favoured octahedral geometry.

The reaction of $[\text{TaCl}_5]$ with 0.5 equivalents of *p*-tert-butylcalix[8]arene H_8 ($\text{H}_8t\text{Bu-L}^1$) in refluxing dichloromethane afforded, after work-up, yellow prisms of $[(\text{TaCl}_2)_2(t\text{Bu-L}^1\text{H}_2)]$ (**5**) in good yield (about 50%). As for **1**, **2** and **4**, complex **5** is formed stoichiometrically by loss of three equivalents of HCl per metal centre. The IR spectrum of

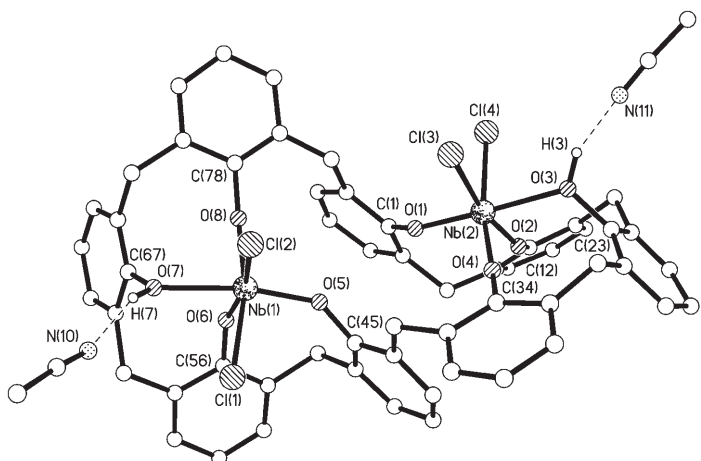


Figure 4. Molecular structure of **4**. Hydrogen atoms, except OH, and calixarene *t*Bu groups omitted for clarity. Selected bond lengths [Å] and angles [°]: Nb(1)–Cl(1) 2.402(4), Nb(1)–Cl(2) 2.412(4), Nb(1)–O(5) 1.873(9), Nb(1)–O(6) 1.884(10), Nb(1)–O(7) 2.227(9), Nb(1)–O(8) 1.855(10); Cl(1)–Nb(1)–Cl(2) 87.31(14), C(45)–O(5)–Nb(1) 142.7(8), C(56)–O(6)–Nb(1) 143.8(10), C(67)–O(7)–Nb(1) 114.4(8), C(78)–O(8)–Nb(1) 161.7(8). Data presented for one of the four molecules in the asymmetric unit; the geometry of the others is similar.

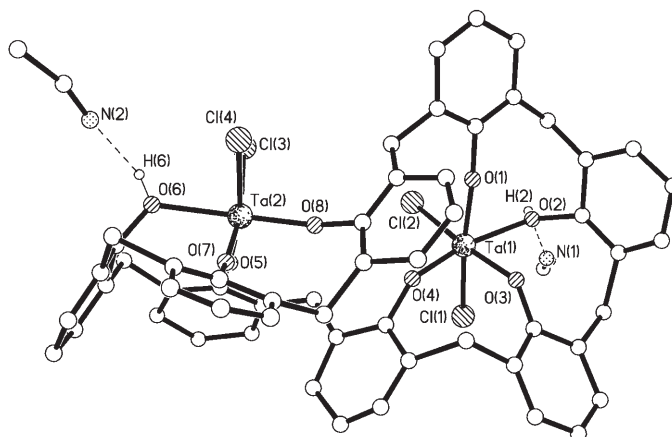


Figure 5. Molecular structure of **5**. Hydrogen atoms and calixarene *t*Bu groups omitted for clarity.

shown in Figure 6, with selected bond lengths and angles given in the caption. The complex is trimeric with niobium-oxacalix[3]arene fragments linked through asymmetric oxo-

this compound contains a broad feature at 3164 cm^{-1} assigned to $\nu(\text{O}-\text{H})$. The ^1H NMR spectrum is consistent with the solid-state structure (see Supporting Information, section a, part v for full spectrum). As for **4**, the *endo* methylene protons appear as four doublets between $\delta=4.43$ – 5.45 ppm (each integrating to 2H), the *exo* protons as two doublets at $\delta=3.43$ and 3.45 ppm (each integrating to 2H) together with a singlet at $\delta=2.97$ ppm (4H); a broad singlet (integrating to 2H) appears at $\delta_{\text{OH}}=9.76$ ppm. As for **1** and **2**, DFQ-COSY experiments revealed the connectivity of the CH_2 groups (see Supporting Information, section a, vii). In the ^{13}C NMR spectra of **3** and **4**, four ArCH_2Ar resonance signals were found between $\delta=32.6$ and 34.4 ppm. Crystals only suitable for a preliminary X-ray diffraction study by using synchrotron radiation were grown from a saturated acetonitrile solution on prolonged standing at ambient temperature. The diffraction was weak, however, it was clear that **5** was isostructural with the $P2_1$ form of **4** containing four molecules of the complex and approximately 27 acetonitrile molecules of crystallisation in the unit cell. Figure 5 shows the molecular structure of **5**, though because of the weak data we have not discussed any geometrical parameters here.

Use of *p*-tert-butylhexahomotrioxacalix[3]areneH₃ (H₃*t*Bu-L²): Reaction of $[\text{NbOCl}_3]$ with Li_3L^2 (generated in situ from H_3L^2 and 3.2 equivalents of MeLi) affords, following work-up, pale yellow crystalline $[\{\text{Nb}(\textit{t}\text{Bu-L}^2)(\mu\text{-O})\}_3](\mathbf{6})$ with a poor yield (ca. 25%). The IR spectrum of this complex contained strong bands in the 600 – 800 cm^{-1} region consistent with $\nu(\text{Nb}-\text{O}-\text{Nb})$ vibrations of bridging oxo groups. Small single crystals suitable for an X-ray study by using synchrotron radiation^[19] were grown from a saturated solution of **6** in acetonitrile at 0°C . The molecular structure is

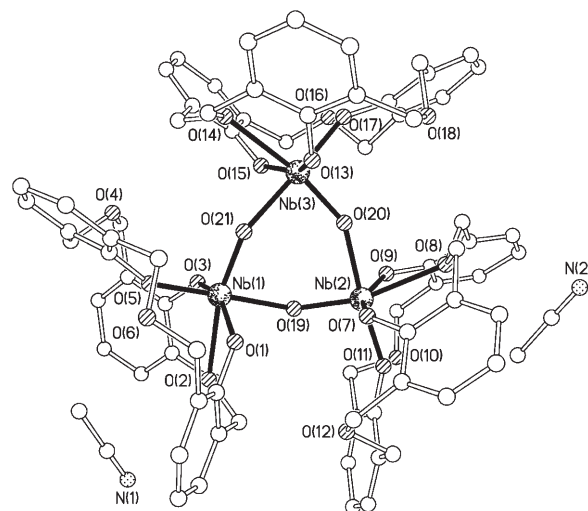


Figure 6. Molecular structure of **6**. Hydrogen atoms and calixarene *t*Bu groups omitted for clarity. Selected bond lengths [Å] and angles [°]: Nb(1)–O(1) 1.934(5), Nb(1)–O(2) 2.404(5), Nb(1)–O(3) 1.905(5), Nb(1)–O(5) 1.897(6), Nb(1)–O(21) 1.811(5), Nb(3)–O(21) 2.072(5); O(19)–Nb(1)–O(21) 87.4(2), Nb(1)–O(21)–Nb(3) 146.6(3).

bridges. The result is a central, slightly puckered, Nb_3O_3 metalocyclic ring. Each niobium centre is pseudo-octahedral, the sixth site being occupied via donation ($\text{Nb}-\text{O}$ ca. 2.39 Å) from an oxygen of one of the dimethyleneoxa bridges; the latter are *trans* to the shorter of the μ -oxo bridges.

The central Nb_3O_3 core is similar to that reported by Cotton and co-workers for the complex $[\{\text{NbOCl}_3(\text{OCRR}')\}_3]$ ($\text{R}=\text{C}_6\text{H}_5$, $\text{R}'=m\text{-Me-C}_6\text{H}_4$).^[29]

Similar reaction of $[\text{TaOCl}_3]$ and $\text{Li}_3(\textit{t}\text{Bu-L}^2)$ affords $[\{\text{Ta}(\textit{t}\text{Bu-L}^2)(\mu\text{-O})\}_3](\mathbf{7})$ with a poor yield (ca. 15%). Spectro-

scopic characterisation indicates that **7** adopts an analogous trimeric structure to that adopted by **6**.

Use of *p*-tert-butylcalix[4]areneH₄ and 1,3-dimethoxy-*p*-tert-butylcalix[4]areneH₂: The dinuclear complexes $[(MCl)p\text{-tert-butylcalix[4]arene}]_2$ ($M = Nb$ (**8**), Ta (**9**)) were prepared as reported previously.^[4] The monomeric complex $[(NbCl_2)p\text{-tert-butylcalix[4]arene(OMe)}]$ (**10**) was prepared by using the same procedure as reported for the analogous known tantalum complex (**11**).^[4] The ¹H NMR spectrum is consistent with C_s symmetry with four doublets for the ArCH₂Ar resonances, together with a ratio of 2:1:1 for the *tert*-butyl groups. The OMe resonance appears as a singlet at $\delta = 3.91$ ppm. In the ¹³C NMR spectrum, two ArCH₂Ar resonances appear at $\delta = 34.4$ and 34.9 ppm, with the OMe group appearing at $\delta = 69.7$ ppm. Single crystals of **10** suitable for an X-ray structure determination (see Figure 7) by

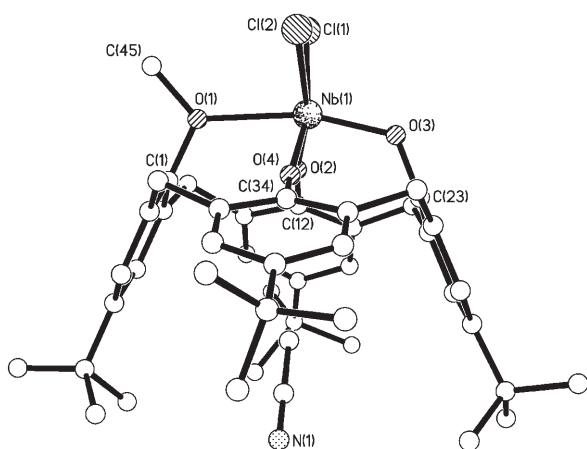


Figure 7. Molecular structure of **10**-MeCN. Hydrogen atoms omitted for clarity.

using synchrotron radiation^[19] were grown from a saturated solution of **10** in acetonitrile on prolonged standing (2–3 days) at ambient temperature. There are 1.5 molecules of **10**-MeCN in the asymmetric unit, with that containing Nb(1) in a general position, whilst that containing Nb(2) lies on a mirror plane. Both molecules are monomeric with pseudo-octahedral niobium centres and methoxycalix[4]arene ligands adopting what can best be described as a pinched conformation (the distance between centroids of the opposing phenolate rings is 6.30 and 7.50 Å) and with the methoxymethyl group pointing away from the cavity; a similar structure was observed for the toluene solvates $[(TaCl_2)p\text{-tert-butylcalix[4]arene(OMe)}]$,^[4] and $[(NbCl_2)p\text{-tert-butylcalix[4]arene(OMe)}]$,^[5] the geometrical parameters of this latter solvate and our acetonitrile solvate are compared in Table 2. In **10**, each niobium is displaced by about 0.22 Å above the plane defined by O(2), O(4), Cl(1) and Cl(2), whilst there is severe distortion of the “plane” defined by the four oxygen atoms bound to the lower rim of the methoxycalix[4]arene. The Nb–Cl distances (Nb(1)–Cl(1) 2.3872(14) and Nb(1)–Cl(2) 2.3904(14) Å) are close to those

Table 2. Comparison of selected bond lengths [Å] and angles [°] for **10**-MeCN and **10**-toluene.^[5]

	MeCN	Toluene
Nb(1)–O(1)	2.300(3)	2.259(2)
Nb(1)–O(2)	1.849(3)	1.841(3)
Nb(1)–O(3)	1.877(3)	1.917(2)
Nb(1)–O(4)	1.863(3)	1.862(2)
Nb(1)–Cl(1)	2.3872(14)	2.359(1)
Nb(1)–Cl(2)	2.3904(14)	2.396(1)
Nb(1)–O(1)–C(1)	117.4(3)	117.88(19)
Nb(1)–O(2)–C(12)	171.6(3)	170.9(2)
Nb(1)–O(3)–C(23)	124.3(3)	120.8(2)
Nb(1)–O(4)–C(34)	154.7(3)	153.2(2)
Cl(1)–Nb(1)–Cl(2)	86.27(5)	

observed in **1**. As expected, the Nb(1)–O(1) ether linkage (2.300(3) Å) is somewhat longer than that to the aryloxy oxygen atoms (1.849(3)–1.877(3) Å), whilst the Nb–O–C angles at O(2) and O(4) (171.6(3) and 154.7(3)°, respectively) are considerably larger than those at O(1) and O(3) (128.6(3) and 124.3(3)°, respectively), reflecting the differing degrees of π donation. Each acetonitrile molecule of crystallisation resides just inside of one of the calixarene cones; there is evidence of a second very-low-occupancy set of positions for C(73) and N(1) lying along the other side of the pinched cone (this was not modelled), whilst that containing N(2) is split 50/50 in two orientations.

Catalytic screening: The pro-catalysts **1–11** (apart from **3**) (see Scheme 3) have been screened for their ability to polymerise ethylene in the presence of a number of organoaluminium co-catalysts (see Tables 3, 4 and 5).

In the presence of either dimethylaluminium chloride (DMAC) or diethylaluminium chloride (DEAC), and the re-activating substance ethyl trichloroacetate (ETA), all of the catalytic systems exhibit poor-to-moderate activity, as defined by the Gibson criteria,^[7a] for the polymerisation of ethylene. High-molecular-weight, solid polyethylene is obtained in all cases; melting points (132–135°C) obtained by using differential scanning calorimetry (DSC) are typical for linear polyethylene. The nature of the co-catalyst is crucial, for example, for pro-catalyst **1** with methylaluminumoxane (MAO) or trimethylaluminium (TMA), the activity is poor (≤ 1 g mmol⁻¹ h⁻¹ bar⁻¹, runs 6 and 7), whereas the use of DMAC (20 g mmol⁻¹ h⁻¹ bar⁻¹, run 1) or DEAC (32 g mmol⁻¹ h⁻¹ bar⁻¹, run 8) leads to an observed increase in the activity. We have noted such co-catalyst effects in other systems.^[35] In no case has polyethylene been obtained in the absence of organoaluminium co-catalyst. The presence of ETA seems to inhibit the catalytic activity of MAO (compare runs 6 and 9), whereas for DMAC and DEAC the presence of ETA led to increased catalytic activity. The catalytic activity of the system when using **1–5** (but not using **3**) as pro-catalyst is a function of the [Al]:[Nb] molar ratio, increasing with increased excess of DMAC or DEAC (we have gone as high as 600 molar equivalents of DMAC), see Supporting Information, section b, i. There is also a clear dependence of activity on the temperature of the catalytic run

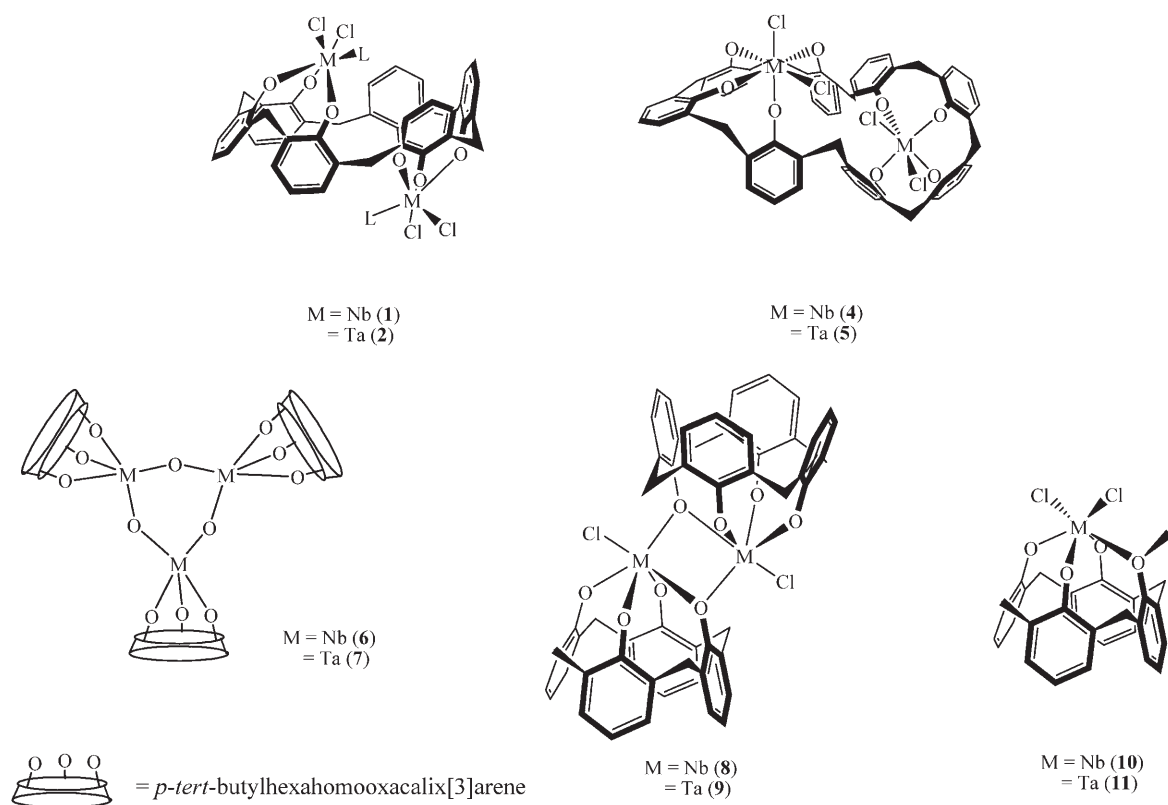
Scheme 3. Niobium- and tantalum-based calixarene pro-catalysts screened in this study (calixarene *t*Bu groups removed for clarity).

Table 3. Polyethylene runs for niobium pro-catalysts at 45 °C.

Run no	Catalyst system	Yield PE [mg]	Activity	M_w	M_n	M_w/M_n
1	1	196	20	319000	135000	2.4
2	4	186	19	324000	145000	2.2
3	8	87	9	391000	169000	2.3
4	10	98	20	436000	184000	2.4
5	6	442	84	296000	119000	2.5

Table 4. Variation of co-catalyst and use of re-activator with **1**.^[a]

Run no	Co-catalyst	ETA [mL]	Yield PE [mg]	Activity	PE M.p. [°C]
6	MAO	0.1	7	1	130
7	TMA	0.1	9	1	132
1	DMAC	0.1	196	20	133
8	DEAC	0.1	320	32	133
9	MAO	0	63	6	133
10	TMA	0	3	trace	131
11	DMAC	0	10	1	132
12	DEAC	0	3	trace	133

[a] All runs completed with 10 μ mol of pro-catalyst, 300 equivalents of co-catalyst, and a pressure of 1 bar ethylene, for 30 min, at 45 °C.

for the methylene-bridged calixarene systems, with the activity peaking at around 45 °C with DMAC and at about 25 °C with DEAC (see Supporting Information, section b, ii).

Table 5. Polyethylene runs for tantalum pro-catalysts.^[a]

Run no	Catalyst system	Yield PE [mg]	Activity	M_w	M_n	M_w/M_n
13	2	325	33	167000	67800	2.5
14	5	88	9	253000	104000	2.4
15	9	138	14	306000	117000	2.6
16	11	47	9	301000	111000	2.7
16	7	229	46	338000	123000	2.0
17	2 ^[b]	33	3	–	–	–
18	2 ^[b]	137	13	–	–	–

[a] All runs completed with 10 μ mol of pro-catalyst, 300 equivalents of DMAC and 0.1 mL of ETA under a pressure of 1 bar ethylene, for 30 min, at 60 °C. [b] By using 300 equivalents of DEAC.

In the presence of DEAC and ETA, the molecular weights of the polymers produced are remarkably similar (100000–200000), whereas for DMAC with ETA molecular weights are somewhat higher (319000–436000). The polydispersities (M_w/M_n) are generally in the range 2.2–2.4. For the (-CH₂OCH₂-)-bridged pro-catalyst system **6**, there is an increased observed activity (84 g mmol⁻¹h⁻¹bar⁻¹, run 5), which falls to <20 g mmol⁻¹h⁻¹bar⁻¹ on increasing the temperature to 80 °C.

In the literature, there is a general trend for tantalum pro-catalysts to have higher activities than those of their niobium counterparts, however this was not found to be the case for the systems described herein. The tantalum calixarenes (Table 5) produced similar high-molecular-weight polyethy-

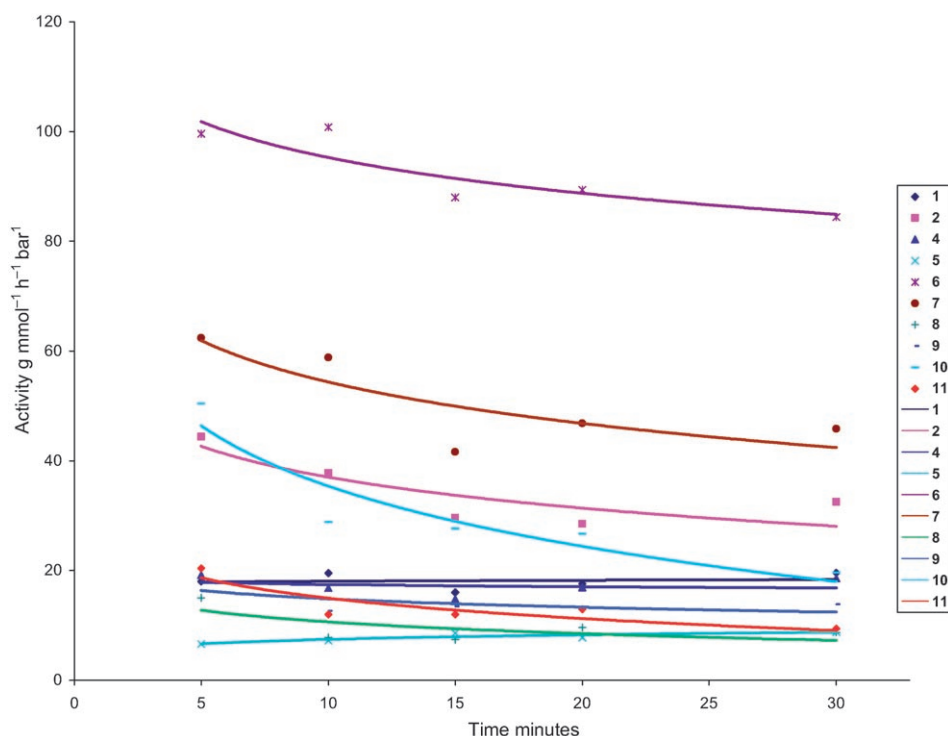


Figure 8. Lifetimes of catalyst systems at 300 equivalents co-catalyst, 10 mmol pro-catalyst, 0.1 mL reactivator (45°C for niobium catalysts, 60°C for tantalum catalysts).

lene with polydispersities close to those observed for the niobium calixarenes. As for niobium, the use of DMAC versus MAO was beneficial for observed catalytic activity. Similarly, the pro-catalyst **7** containing the (-CH₂OCH₂-) bridged ligand system has the highest observed catalytic activity (46 g mmol⁻¹h⁻¹bar⁻¹, run 16), which falls to <1 g mmol⁻¹h⁻¹bar⁻¹ on increasing the temperature to 80°C. Over 30 min, the observed activities of these niobium/tantalum catalysts remains fairly constant (see Figure 8, and Supporting Information, section b, iii).

Conclusion

We have synthesised and characterised novel niobium(V) and tantalum(V) calix[*n*]arene (*n*=6 and 8) complexes from reactions of the parent ligands with either [MCl₃] (M=Nb, Ta) or [NbOCl₃]. These complexes, when activated with either MAO, TMA, DMAC or DEAC, either with or without ETA present, display poor-to-moderate activity (<35 g mmol⁻¹h⁻¹bar⁻¹) for the polymerisation of ethylene, doubtless due to the instability associated with the metal-alkyl cations present.^[36] [MOCl₃] (M=Nb, Ta) reacts with the tri-lithium salt of *p*-*tert*-butylhexahomotrioxacalix[3]arene, H₃*t*Bu-L², to afford trimeric complexes of the form [(M-(*t*Bu-L²)(μ-O))₃]. When activated with the combination of either DMAC or DEAC and ETA, under the same condi-

tions as those employed for the methylene-bridged systems, these complexes containing CH₂OCH₂-bridged ligands, display slightly higher catalytic activity (Nb, 84 g mmol⁻¹h⁻¹bar⁻¹; Ta, 46 g mmol⁻¹h⁻¹bar⁻¹), an activity trend which, although less pronounced, mimics that observed previously for vanadyl calixarene/oxacalixarene-based catalysis.^[3]

Owing to the rather low activities displayed by the pro-catalysts described herein, further catalytic studies of this type using niobium- and tantalum-based systems have been discontinued. However, these calix[*n*]arene (*n*=6 and 8) complexes do have potential, via metal-metal bond formation, to mediate a number of useful transformations (see, for example, the calix[4]arene chemistry of the Floriani group);^[4] such studies are currently in progress.

Experimental Section

All manipulations were carried out under an atmosphere of nitrogen by using standard Schlenk and cannula techniques or in a conventional nitrogen-filled glove-box. Solvents were refluxed over an appropriate drying agent, and were distilled and degassed prior to use. Elemental analyses were performed by the microanalytical services of the School of Chemical Sciences and Pharmacy at The University of East Anglia, by Medac Ltd and by Mr Stephen Boyer at London Metropolitan University. ¹H NMR spectra were recorded by using a Varian Inora 600 or a Varian VXR 400 S spectrometer at either 273 or 298 K; chemical shifts were referenced to the residual protio impurity of the deuterated solvent. Standard DEPT-135 experiments were used to distinguish -CH₃ and -CH type carbons from -C- or -CH₂-type carbons in the ¹³C NMR spectra, which were recorded by using a Bruker Avance DPX 300 spectrometer. IR spectra (Nujol mulls, KBr/CsI windows) were recorded by using either a Perkin-Elmer 577 or a 457 grating spectrophotometer. [MOCl₃] was made by the method of Gibson.^[30] The ligands H₃*t*Bu-L² and 1,3-dimethoxy-*p*-*tert*-butylcalix[4]areneH₂ were prepared by using methods in the literature.^[31,32] All other chemicals were obtained commercially and used as received unless stated otherwise.

[(Nb(NCMe)Cl₂)₂(*t*Bu-L)] (1): From [NbCl₃]: [NbCl₃] (0.580 g, 2.15 mmol) and H₃*t*Bu-L (1.00 g, 1.03 mmol) were combined in a Schlenk flask in a dry-box. Toluene (30 mL) was added and the system was refluxed for 12 h to afford an orange suspension. Following removal of volatiles in vacuo, the residue was extracted, by using a frit, into hot acetonitrile (3 × 30 mL). The orange/red solid remaining on the frit was dried in vacuo (0.940 g, 66.3%). M.p. 201 °C (decomp); ¹H NMR (600 MHz, CDCl₃, 273 K): δ = 7.55 (1H; aryl H), 7.54 (d, ⁴J(H,H)=1.2 Hz, 2H; aryl H), 7.44 (d, ⁴J(H,H)=1.8 Hz, 1H; aryl H), 7.40 (m, ⁴J(H,H)=1.2 Hz, 1H; aryl H), 7.36 (d, ⁴J(H,H)=2.4 Hz, 1H; aryl H), 7.28 (s, 1H; aryl H), 7.26 (m, partially obscured by solvent, 2H; aryl H), 7.20 (d, ⁴J(H,H)=

1.8 Hz, 1H; aryl H), 7.18 (d, $^4J(\text{H,H})=2.4$ Hz, 1H; aryl H), 6.96 (d, $^4J(\text{H,H})=0.6$ Hz, 1H; aryl H), 6.95 (d, $^4J(\text{H,H})=0.6$ Hz, 1H; aryl H), 5.38 (d, $^2J(\text{H,H})=12.6$ Hz, 1H; *endo-CH₂*), 5.24 (d, $^2J(\text{H,H})=13.8$ Hz, 1H; *endo-CH₂*), 5.22 (d, $^2J(\text{H,H})=13.8$ Hz, 1H; *endo-CH₂*), 5.13 (d, $^2J(\text{H,H})=12.6$ Hz, 1H; *endo-CH₂*), 4.65–4.62 (d + s, $^2J(\text{H,H})$ =observed, 3H; *endolexo-CH₂*), 4.56 (d, $^2J(\text{H,H})=17.4$ Hz, 1H; *exo-CH₂*), 3.81 (d, $^2J(\text{H,H})=13.2$ Hz, 2H; *exo-CH₂*), 3.76 (d, $^2J(\text{H,H})=13.2$ Hz, 2H; *exo-CH₂*), 2.90 (sbr, 2H; 2/3MeCN), 2.31 (sbr, 6H; MeCN), 1.53 (s, 18H; C-(CH₃)₃), 1.48 (s, 9H; C(CH₃)₃), 1.45 (s, 9H; C(CH₃)₃), 1.41 (s, 18H; C-(CH₃)₃), 0.36 ppm (sbr, 2H; 2/3MeCN); ¹³C NMR (CDCl₃, 75 MHz): $\delta=161.8, 159.5, 158.0$ (all aryl-C), 147.4, 146.9, 146.3 (all aryl-C_p), 135.8, 134.5, 132.9, 130.2, 129.6 (all aryl-C_o), 127.1, 126.8, 126.3 (all aryl-C_m), 125.7 (aryl-C_o), 125.5, 124.7, 124.3 (all aryl-C_m), 121.6, 120.6, 116.4 (all MeCN), 34.7 (C(CH₃)₃), other C_{quat} are not seen, 34.4, 34.2, 33.3 (all CH₂), 31.9, 31.8, 31.7 (all C(CH₃)₃), 3.5, 1.8, -3.3 ppm (MeCN); IR: $\tilde{\nu}=2310$ (w), 2281 (w), 2279 (w), 1654 (w), 1588 (w), 1379 (s), 1281 (m), 1275 (m), 1272 (m), 1260 (s), 1255 (s), 1206 (s), 1096 (s), 1091 (s), 1020 (s), 922 (s), 886 (s), 855 (m), 845 (s), 799 (s), 764 (m), 630 cm⁻¹ (w); elemental analysis calcd (%) for Nb₂Cl₄N₂O₆C₇₀H₈₄: C 61.1, H 6.1, N 2.0; found: C 60.8, H 6.1, N 2.0. Small crystals suitable for X-ray crystallography by using synchrotron radiation were obtained from a saturated acetonitrile solution on prolonged standing (2–3 days) at room temperature. Use of acetonitrile as sole solvent (for reaction and crystallisation) led to oilier products.

From [NbOCl₃]: [NbOCl₃] (1.00 g, 4.60 mmol) and H₈tBu-L (2.23 g, 2.30 mmol) were combined in a Schlenk flask, toluene (40 mL) was added and the system was refluxed for 12 h. On cooling, volatiles were removed in vacuo and the residue was extracted into warm MeCN (30 mL). Prolonged standing (2–3 days) at room temperature afforded orange **1** (0.47 g, 15%) and pale yellow prisms of [(Nb₂(μ-O)₂(μ-Cl)-(tBuLH))₂] (**3**) (0.31 g, 10%). M.p. 286 °C (decomp); IR: $\tilde{\nu}=3150$ (mbr), 1604 (w), 1301 (mbr), 1261 (s), 1202 (m), 1096 (sbr), 1020 (sbr), 920 (w), 873 (m), 799 (s), 722 (m), 680 cm⁻¹ (w); elemental analysis calcd (%) for Nb₄Cl₂O₁₆C₁₃₂H₁₅₈6MeCN: C 64.3, H 6.6, N 3.1; found: C 64.4, H 6.7, N 3.1. The poor solubility of **3** precluded further spectroscopic characterisation.

[[Ta(NCMe)Cl₃]₂(tBu-L)] (2**):** [TaCl₅] (1.00 g, 2.80 mmol) and H₈tBu-L (1.36 g, 1.40 mmol) were combined in a dry-box. Dichloromethane (30 mL) was added and the system was refluxed (12 h) to afford a yellow suspension. Following removal of volatiles in vacuo, the residue was extracted into warm MeCN (30 mL). On prolonged standing (1 week) at -10 °C, complex **2** formed as pale yellow needles (1.13 g, 49.5%). M.p. 220 °C (decomp); ¹H NMR (600 MHz, CDCl₃, 273 K): $\delta=7.19$ (d, $^4J(\text{H,H})$ =not observed, 1H; aryl H), 7.17 (d, $^4J(\text{H,H})$ =not observed, 2H; aryl H), 7.13 (d, $^4J(\text{H,H})$ =not observed, 1H; aryl H), 7.09 (d, $^4J(\text{H,H})$ =not observed, 1H; aryl H), 7.01 (d, $^4J(\text{H,H})$ =not observed, 1H; aryl H), 6.98 (d, $^4J(\text{H,H})$ =not observed, 2H; aryl H), 6.95 (d, $^4J(\text{H,H})$ =not observed, 1H; aryl H), 6.86 (d, $^4J(\text{H,H})$ =not observed, 1H; aryl H), 6.66 (d, $^4J(\text{H,H})=6.9$ Hz, 2H; aryl H), 5.02 (d, $^2J(\text{H,H})=13.2$ Hz, 1H; *endo-CH₂*), 4.90 (d, $^2J(\text{H,H})=13.8$ Hz, 1H; *endo-CH₂*), 4.89 (d, $^2J(\text{H,H})=13.8$ Hz, 1H; *endo-CH₂*), 4.77 (d, $^2J(\text{H,H})=12.6$ Hz, 1H; *endo-CH₂*), 4.30–4.27 (d + s, $^2J(\text{H,H})$ =observed, 3H; *endolexo-CH₂*), 4.21 (d, $^2J(\text{H,H})=13.2$ Hz, 1H; *exo-CH₂*), 3.52 (d, $^2J(\text{H,H})=13.8$ Hz, 2H; *exo-CH₂*), 3.48 (d, $^2J(\text{H,H})=13.8$ Hz, 1H; *exo-CH₂*), 3.46 (d, $^2J(\text{H,H})=12.6$ Hz, 1H; *exo-CH₂*), 2.50 (1/2 MeCN), 2.01 (3 MeCN), 1.24 (s, 18H; C-(CH₃)₃), 1.18 (s, 9H; C(CH₃)₃), 1.12 (s, 9H; C(CH₃)₃), 1.11 (s, 18H; C-(CH₃)₃), -0.36 ppm (1/2 MeCN); ¹³C NMR (CDCl₃, 75 MHz): $\delta=156.8, 155.9, 155.6, 155.4, 154.8$ (all aryl-C), 148.8, 147.8, 146.5, 146.4, 146.2, 146.1 (aryl-C_p), 134.2, 134.1, 133.9, 132.9, 132.8, 130.7, 129.9, 128.5, 128.4, 127.3, 127.2 (all aryl-C_o), 126.5, 126.1, 125.7, 124.9, 124.9, 124.8, 124.4, 124.2, 123.6, 123.5 (all aryl-C_m), 121.8, 121.2, 116.4 (all MeCN), 34.5, 34.5, 34.2, 34.1, 34.1 (C(CH₃)₃), 33.7, 33.5, 32.6 (all CH₂), 31.5, 31.4, 31.3, 31.3 (all C(CH₃)₃), 3.7, 1.9, -3.4 ppm (all MeCN); IR: $\tilde{\nu}=2340$ (w), 2295 (w), 1456 (s), 1411 (w), 1376 (m), 1357 (w), 1260 (s), 1185 (m), 1094 (s), 1018 (s), 927 (w), 858 (w), 798 (s), 764 cm⁻¹ (w); elemental analysis calcd (%) for Ta₂Cl₄N₂O₆C₇₀H₈₄2MeCN: C 54.4, H 5.5, N 3.4; found: C 54.2, H 5.6, N 3.6.

[(NbCl₂)₂(tBu-L¹H₂)] (4**):** As for **1**, but by using [NbCl₅] (1.25 g, 4.63 mmol) and H₈tBu-L¹ (2.98 g, 2.30 mmol) affording **2** as orange prisms (2.15 g, 50.2%). M.p. 192 °C (decomp); ¹H NMR (600 MHz, [D₈]toluene): $\delta=9.79$ (s, 2H; OH), 7.50 (d, $^4J(\text{H,H})=2.4$ Hz, 2H; aryl H), 7.38 (d, $^4J(\text{H,H})=2.4$ Hz, 2H; aryl H), 7.34 (d, $^4J(\text{H,H})=2.4$ Hz, 2H; aryl H), 7.30 (d, $^4J(\text{H,H})=1.8$ Hz, 4H; aryl H), 7.22 (d, $^4J(\text{H,H})=1.2$ Hz, 2H; aryl H), 7.19 (m, *J* is obscured by solvent, 2H; aryl H), 6.69 (d, $^4J(\text{H,H})=1.2$ Hz, 2H; aryl H), 5.57 (d, $^2J(\text{H,H})=17.5$ Hz, 2H; *endo-CH₂*), 5.17 (d, $^2J(\text{H,H})=14.0$ Hz, 2H; *endo-CH₂*), 4.90 (d, $^2J(\text{H,H})=14.5$ Hz, 2H; *endo-CH₂*), 4.62 (d, $^2J(\text{H,H})=17.5$ Hz, 2H; *endo-CH₂*), 3.52 (d, $^2J(\text{H,H})=14.0$ Hz, 2H; *exo-CH₂*), 3.49 (d, $^2J(\text{H,H})=14.5$ Hz, 2H; *exo-CH₂*), 3.10 (s, 4H; *exo-CH₂*), 2.15 (s, 1.5H; 1/2 MeCN), 1.27 (s, 18H; C-(CH₃)₃), 1.18 (s, 18H; C(CH₃)₃), 1.16 (s, 18H; C(CH₃)₃), 0.87 (s, 18H; C-(CH₃)₃), 0.63 ppm (s, 18H; 6MeCN); ¹³C NMR (C₆D₆, 75 MHz): $\delta=161.5, 161.2, 160.2$ (all aryl-C), 149.8, 149.2, 147.6, 147.3, 146.8, 146.0, 144.9, 133.8, 132.8, 132.7, 131.6, 130.6, 129.4, 129.3, 126.9, 126.1, 125.8, 124.7, 124.6, 123.8 (all aryl-C; 1 signal obscured by solvent), 116.7 (MeCN), 35.5, 34.6, 34.6 (all CH₂), 34.4, 34.3 (both C(CH₃)₃), 33.9 (CH₂), 32.6 (C(CH₃)₃), other C_{quat} not seen, 31.9, 31.7, 31.6, 31.3 (4 × C(CH₃)₃), 0.4 ppm (MeCN); IR: $\tilde{\nu}=3158$ (wbr), 2393 (w), 2342 (w), 1646 (w), 1568 (w), 1302 (m), 1259 (s), 1199 (s), 1113 (s), 1044 (m), 941 (m), 881 (s), 795 (s), 726 (s), 563 cm⁻¹ (m); elemental analysis calcd (%) for Nb₂Cl₄O₈C₈₈H₁₀₆6MeCN: C 64.3, H 6.7, N 4.5; found: C 64.2, H 6.7, 4.2.

[(TaCl₂)₂(tBu-L¹H₂)] (5**):** As for **1**, but by using [TaCl₅] (1.65 g, 4.60 mmol) and H₈tBu-L¹ (2.98 g, 2.30 mmol) affording **5** as golden/yellow prisms on standing (2.02 g, 49%). M.p. 206 °C (decomp); ¹H NMR (600 MHz, C₆D₆): $\delta=10.56$ (sbr, 2H; OH), 7.47 (d, $^4J(\text{H,H})=1.8$ Hz, 2H; aryl H), 7.24 (d, $^4J(\text{H,H})=2.4$ Hz, 2H; aryl H), 7.28 (d, $^4J(\text{H,H})=1.8$ Hz, 2H; aryl H), 7.25 (d, $^4J(\text{H,H})=2.4$ Hz, 2H; aryl H), 7.22 (d, $^4J(\text{H,H})=1.8$ Hz, 2H; aryl H), 7.15 (d, $^4J(\text{H,H})$ =not observed, 2H; aryl H), 7.10 (m, 2H; aryl H), 6.64 (sbr, 2H; aryl H), 5.45 (d, $^2J(\text{H,H})=17.4$ Hz, 2H; *endo-CH₂*), 5.03 (d, $^2J(\text{H,H})=13.8$ Hz, 2H; *endo-CH₂*), 4.85 (d, $^2J(\text{H,H})=14.4$ Hz, 2H; *endo-CH₂*), 4.43 (d, $^2J(\text{H,H})=17.4$ Hz, 2H; *endo-CH₂*), 3.45 (d, 2H; $^2J(\text{H,H})=13.8$ Hz, 2H; *exo-CH₂*), 3.43 (d, $^2J(\text{H,H})=14.4$ Hz, 2H; *exo-CH₂*), 2.97 (s, 4H; *exo-CH₂*), 1.20 (s, 15H; MeCN), 1.13 (s, 18H; C(CH₃)₃), 1.07 (s, 18H; C(CH₃)₃), 0.79 (s, 18H; C-(CH₃)₃), 0.65 ppm (s, 18H; C(CH₃)₃); ¹³C NMR (CDCl₃, 75 MHz): $\delta=158.5, 158.0, 157.9$ (all aryl-C), 149.7, 148.7, 147.3, 147.0, 146.1, 145.4, 133.9, 132.9, 132.1, 131.4, 131.3, 130.2, 129.7, 129.1, 128.3, 128.1, 126.7, 126.4, 126.1, 125.9, 124.6 (all aryl-C), 116.9 (MeCN), 35.5, 34.5 (both CH₂), 34.5, 34.4, 34.3, 34.2 (all C(CH₃)₃), 34.0, 33.6 (both CH₂), 32.0, 31.8, 31.6, 31.4 (all C(CH₃)₃), 0.4 ppm (MeCN); IR: $\tilde{\nu}=3165$ (wbr), 2357 (wbr), 1748 (s), 1596 (w), 1299 (s), 1254 (s), 1207 (s), 1118 (s), 1108 (m), 1024 (w), 994 (w), 937 (m), 878 (m), 861 (m), 823 (w), 794 (w), 758 (w), 739 (w), 728 (w), 674 (w), 668 cm⁻¹ (w); elemental analysis calcd (%) for Ta₂Cl₄O₈C₈₈H₁₀₆5MeCN: C 58.8, H 6.1, N 3.5; found: C 59.0, H 6.2, N 3.8.

[[Nb(tBu-L²)(μ-O)]₃] (6**):** MeLi (4.10 mL, 1.59 M in hexanes, 6.52 mmol) was added to H₃L² (1.14 g, 1.98 mmol) in diethyl ether (40 mL) at -78 °C. The solution was warmed to room temperature and was stirred for 6 h. The solvent was removed in vacuo, toluene (40 mL) and [NbOCl₃] (0.51 g, 2.38 mmol) were added and the system was stirred at room temperature overnight. The solution was filtered to remove LiCl, the solvent was removed in vacuo and **6** was recrystallised from MeCN (0 °C), (0.33 g, 23.4%). M.p. 280 °C (decomp); ¹H NMR (C₆D₆, 400 MHz): $\delta=7.14$ (m, 9H; aryl H), 7.07 (m, 9H; aryl H), 5.89 (sbr, 6H; CH₂), 5.03 (d, $J(\text{H,H})=11.5$ Hz, 6H; CH₂), 4.42–4.36 (s and d, $J(\text{H,H})=7.9$ Hz, 12H; CH₂), 4.11 (d, $J(\text{H,H})=11.5$ Hz, 6H; CH₂), 4.02 (d, $J(\text{H,H})=11.0$ Hz, 6H; CH₂), 1.25 (s, 27H; C(CH₃)₃), 1.20 (s, 54H; C-(CH₃)₃), 0.29 ppm (s, 9H; 3MeCN); IR: $\tilde{\nu}=3382$ (m), 3149 (m), 2961 (s), 2349 (w), 2330 (w), 1623 (w), 1481 (m), 1399 (m), 1308 (w), 1261 (s), 1818 (m), 1083 (s), 1023 (s), 881 (w), 846 (w), 811 cm⁻¹ (s); MS (ES): 2046 [M⁺]; elemental analysis calcd (%) for C₁₀₈H₁₃₅Nb₃O₂₁ (sample dried for 12 h in vacuo): C 63.3, H 6.6; found: C 63.0, H 6.4.

[[Ta(tBu-L²)(μ-O)]₃] (7**):** As for **6**, but by using [TaOCl₃] (0.420 g, 1.38 mmol) and Li₃L² (1.32 mmol) affording **7** as a pale-yellow solid (0.64 g, 15.5%). M.p. 225 °C (decomp); ¹H NMR (400 MHz, C₆D₆): $\delta=7.20$ –6.20 (m, 18H; aryl H), 5.74 (d, $J(\text{H,H})=9.1$ Hz, 6H; CH₂), 4.12 (d,

$J(\text{H,H})=7.5$ Hz, 6H; CH_2), 4.06 (d, $J(\text{H,H})=13.0$ Hz, 6H; CH_2), 3.84 (d, $J(\text{H,H})=9.1$ Hz, 6H; CH_2), 3.53 (d, $J(\text{H,H})=13.0$ Hz, 6H; CH_2), 3.21 (d, $J(\text{H,H})=7.5$ Hz, 6H; CH_2), 1.12 (s, 27H; $\text{C}(\text{CH}_3)_3$), 1.04 (s, 27H; $\text{C}(\text{CH}_3)_3$), 1.00 ppm (s, 27H; $\text{C}(\text{CH}_3)_3$); IR: $\tilde{\nu}=1607$ (m), 1561 (m), 1308 (s), 1260 (m), 1219 (m), 1126 (m), 1099 (m), 1040 (m), 985 (m), 970 (w), 924 (w), 880 (s), 830 (m), 802 (m), 755 (m), 727 (m), 694 (m), 665 cm^{-1} (m); elemental analysis calcd (%) for $\text{C}_{108}\text{H}_{135}\text{Ta}_3\text{O}_{21}\cdot 9\text{C}_7\text{H}_8$: C 65.4, H 6.6; found: C 65.4, H 7.1.

[(NbCl₅)*p*-*tert*-butylcalix[4]arene(OMe)(NCMe)] (**10**): [NbCl₅] (1.25 g, 4.63 mmol) and 1,3-dimethoxy-*p*-*tert*-butylcalix[4]areneH₂ (2.97 g, 4.39 mmol) were refluxed in toluene (30 mL) for 24 h. Following removal of volatiles in vacuo, the resulting orange residue was washed with hexane (2 × 20 mL) and dried in vacuo. Large orange/red prisms were obtained on prolonged standing (24 h) of a saturated solution in acetonitrile at room temperature (0.974 g, 27.1%). M.p. 193 °C (decomp); ¹H NMR (400 MHz, C₆D₆): $\delta=7.10$ (m, 4H; aryl H), 6.76 (m, 4H; aryl H), 4.93 (d, ² $J(\text{H,H})=13.8$ Hz, 2H; *endo*-CH₂), 4.41 (d, ² $J(\text{H,H})=13.2$ Hz, 2H; *endo*-CH₂), 3.91 (s, 3H; OMe), 3.19 (d, ² $J(\text{H,H})=13.8$ Hz, 2H; *exo*-CH₂), 3.09 (d, ² $J(\text{H,H})=13.2$ Hz, 2H; *exo*-CH₂), 1.28 (s, 18H; $\text{C}(\text{CH}_3)_3$), 0.68 (s, 9H; $\text{C}(\text{CH}_3)_3$), 0.63 (s, 9H; $\text{C}(\text{CH}_3)_3$), 0.54 ppm (s, 3H; MeCN); ¹³C NMR (CDCl₃, 75 MHz): $\delta=166.2$, 160.2, 155.0 (all aryl-C), 146.7, 147.2, 147.1 (all aryl-C_p), 136.0, 133.0, 132.7, 129.5 (all aryl-C_o), 127.5, 126.7 (all aryl-C_m), 126.1 (MeCN), 125.5, 124.5 (aryl-C_m), 116.2 (MeCN), 69.7 (OMe), 34.9, 34.4 (CH₂), 34.3, 34.0, 33.9, (C(CH₃)₃), 32.0, 31.0, 30.7 (C(CH₃)₃), 1.6 (MeCN), 0.2 ppm (MeCN); elemental analysis calcd (%) for C₄₅H₅₅NbCl₂O₄ (sample dried for 12 h in vacuo leading to loss of acetonitrile): C 66.3, H 6.9; found: C 65.8, H 6.7.

Crystallography: Crystal data were collected by using a Bruker Apex 2 CCD diffractometer by using narrow-slice 0.3° ω scans (Bruker SMART 1K for **1** and **4**, Bruker SMART 1000 for **3**). Data for **1** and **2** were collected at Daresbury Laboratory SRS Station 9.8 (16.2 SMX for **6** and **10**) by using silicon-111-monochromated X radiation. Data were cor-

rected for Lp effects and for absorption, based on repeated and symmetry equivalent reflections, and solved by direct methods (Patterson synthesis for **1** and **4**). Structures were refined by full-matrix least-squares on F^2 . Hydrogen atoms were included in a riding model except H(5) in **3** for which coordinates were freely refined. Hydrogen atom U_{iso} values were constrained to be 120% of that of the carrier atom except for methyl-H (150%). All structures exhibited disorder in the *t*Bu groups. This disorder was modelled with two sets of methyl carbon positions with restraints on geometry and anisotropic displacement parameters. MeCN molecules of crystallisation were often disordered and where necessary were either modelled over two sets of positions or as partially occupied. The formula of **3** includes ten very disordered MeCN molecules (five unique) that were modelled as a region of diffuse electron density by the Platon "Squeeze" procedure.^[33] In **3** the largest residual peak lies close to the bridging chloride ion. Compound **10** comprises 1.5 molecules in the asymmetric unit, with the half-molecule lying on a mirror plane. Further details are provided in Table 6. Programs used: Bruker SMART, APEX 2, and Enraf Nonius COLLECT (data collection), Bruker SAINT and DENZO (integration and cell refinement), and SHELXTL (solution, refinement and graphics), and local programs.^[34]

CCDC-624576–CCDC-624581 contain the supplementary crystallographic data for this paper. These data can be obtained free of charge from The Cambridge Crystallographic Data Centre via www.ccdc.cam.ac.uk/data_request/cif.

Acknowledgements

We would like to thank the National Mass Spectrometry Service (Swansea, UK), the EPSRC for studentships to M.R. and D.M.H., the award of beam time at Daresbury Laboratory and for a grant under the INTER-

Table 6. Crystallographic data.

Compound	1·2 MeCN	2·2 MeCN	3·16 MeCN	4·6.75 MeCN	6·2 MeCN	10·MeCN
formula	C ₇₄ H ₉₀ Cl ₄ N ₄ Nb ₂ O ₆	C ₇₄ H ₉₀ Cl ₄ N ₄ Ta ₂ O ₆	C ₁₅₆ H ₂₀₄ Cl ₄ N ₁₆ Nb ₄ O ₁₆	C _{101.5} H _{126.25} Cl ₄ N _{6.75} Nb ₂ O ₈	C ₁₁₂ H ₁₄₁ N ₂ Nb ₃ O ₂₁	C ₄₇ H ₅₈ Cl ₂ NNbO ₄
formula weight	1459.12	1635.20	3072.79	1896.46	2130	864.75
crystal system	triclinic	triclinic	triclinic	monoclinic	monoclinic	orthorhombic
space group	<i>P</i> $\bar{1}$	<i>P</i> $\bar{1}$	<i>P</i> $\bar{1}$	<i>Pn</i>	<i>P</i> ₂ / <i>c</i>	<i>Pnma</i>
unit cell dimensions						
<i>a</i> [Å]	12.8575(9)	12.8347(5)	16.8071(11)	17.0865(6)	16.872(8)	12.4190(13)
<i>b</i> [Å]	13.7228(10)	13.7560(6)	16.9650(11)	43.4357(16)	34.396(16)	56.133(6)
<i>c</i> [Å]	22.4773(16)	22.4619(9)	17.2583(11)	29.4308(10)	19.719(9)	19.628(2)
α [°]	95.482(2)	95.438(2)	100.897(2)	90	90	90
β [°]	103.323(2)	103.264(2)	118.745(2)	98.189(2)	102.687(7)	90
γ [°]	103.526(2)	103.528(2)	90.089(2)	90	90	90
<i>V</i> [Å ³]	3703.2(5)	3706.4(3)	4212.2(5)	21 619(13)	11 164(9)	13 683(2)
<i>Z</i>	2	2	1	8	4	12
λ [Å ³]	0.6861	0.6765	0.71073	0.71073	0.8462	0.8464
<i>T</i> [K]	150(2)	151(2)	150(2)	160(2)	150(2)	150(2)
absorption coefficient, μ [mm ⁻¹]	0.505	3.146	0.389	0.363	0.369	0.422
crystal size [mm]	0.07 × 0.02 × 0.01	0.13 × 0.07 × 0.04	0.80 × 0.63 × 0.20	0.62 × 0.44 × 0.22	0.12 × 0.06 × 0.03	0.16 × 0.08 × 0.03
θ_{max} [°]	29.37	31.06	27.50	25.00	28.07	28.63
reflections measured	39 259	45 564	44 666	173 807	61 908	68 042
unique reflections	20 542	24 168	18 597	74 057	15 958	10 445
reflections with $F^2 > 2\sigma(F^2)$	15 528	21 439	14 786	62 484	8120	7059
transmission factors	0.966–0.995	0.685–0.855	0.746–0.926	0.808–0.924	0.957–0.989	0.936–0.988
R_{int}	0.0482	0.0261	0.0329	0.0986	0.1844	0.1353
number of parameters	901	914	849	4637	1398	857
$R^{\text{[a]}}$ [$F^2 > 2\sigma(F^2)$]	0.0503	0.0315	0.0643	0.1290	0.0686	0.0556
$R_w^{\text{[b]}}$ (all data)	0.1319	0.0817	0.1922	0.2995	0.1835	0.1307
goodness-of-fit ^[c] (<i>S</i>)	1.022	1.054	1.102	1.222	0.951	1.027
largest difference peak and hole [e Å ⁻³]	0.845 and -0.740	1.721 and -1.530	2.979 and -1.766	1.620 and -1.508	0.907 and -0.990	0.448 and -0.588

[a] Conventional $R = \sum ||F_o| - |F_c|| / \sum |F_o|$ for "observed" reflections having $F^2 > 2\sigma(F^2)$. [b] $R_w = [\sum w (F_o^2 - F_c^2)^2 / \sum w (F_o^2)^2]^{1/2}$ for all data. [c] $S = [\sum w (F_o^2 - F_c^2)^2 / (\text{no. of unique reflections} - \text{no. of parameters})]^{1/2}$.

ACT Japan scheme. RAPRA Technology Ltd is thanked for GPC measurements. We acknowledge the use of the EPSRC Chemical Database Service at Daresbury (ref. [27]). We also thank Dr. T. Prior and Dr. J. E. Warren for scientific support at Daresbury Laboratory Stations 9.8 and 16.2 SMX, and Colin MacDonald (UEA) for help with running NMR experiments.

- [1] a) O. V. Ozerov, N. P. Rath, F. T. Ladipo, *J. Organomet. Chem.* **1999**, 586, 223; b) Y. Chen, Y. Zhang, Z. Shen, R. Kou, L. Chen, *Eur. Polym. J.* **2001**, 37, 1181; c) V. C. Gibson, C. Redshaw, M. R. J. Elsegood, *Dalton Trans.* **2001**, 767; d) G. S. Long, B. Snedeker, K. Bartos, M. L. Werner, A. Sen, *Can. J. Chem.* **2001**, 79, 1026; e) C. Capacchione, P. Neri, A. Proto, *Inorg. Chem. Commun.* **2003**, 6, 339; f) M. Frediani, D. Sémeril, A. Comucci, L. Bettucci, P. Frediani, L. Rosi, D. Matt, L. Toupet, W. Kaminsky, *Macromol. Chem. Phys.* **2007**, 208, 938.
- [2] C. Huang, J. Ahn, S. Kwon, J. Kim, J. Lee, Y. Han, H. Kim, *Appl. Catal. A* **2004**, 258, 173.
- [3] C. Redshaw, M. Rowan, L. Warford, D. M. Homden, A. Arbaoui, M. R. J. Elsegood, S. H. Dale, T. Yamato, C. Pérez Casas, S. Matsui, S. Matsuura, *Chem. Eur. J.* **2007**, 13, 1090.
- [4] C. Floriani, R. Floriani-Moro, *Adv. Organomet. Chem.* **2001**, 47, 167.
- [5] S. Dürr, B. Bechlers, U. Radius, *Inorg. Chim. Acta* **2006**, 359, 4215.
- [6] C. Redshaw, *Coord. Chem. Rev.* **2003**, 244, 45.
- [7] a) P. D. Hampton, C. E. Daitch, T. M. Alam, Z. Becze, M. Rosay, *Inorg. Chem.* **1994**, 33, 4750; b) P. D. Hampton, C. E. Daitch, T. M. Alam, Z. Becze, M. Rosay, *Inorg. Chem.* **1997**, 36, 2879; c) B. Masci in *Calixarenes 2001* (Eds.: Z. Asfari, V. Böhmer, J. Harrowfield, J. Vicens), Kluwer, Dordrecht, **2001**, Chapter 12.
- [8] a) G. J. P. Britovsek, V. C. Gibson, D. F. Wass, *Angew. Chem.* **1999**, 111, 448; *Angew. Chem. Int. Ed.* **1999**, 38, 428; b) V. C. Gibson, S. K. Spitzmesser, *Chem. Rev.* **2003**, 103, 283; c) V. C. Gibson, E. L. Marshall, *Comprehensive Coordination Chemistry II, Vol. 9* (Eds.: J. A. McCleverty, T. J. Meyer, M. D. Ward), Elsevier, Amsterdam, **2004**.
- [9] C. Redshaw, D. M. Homden, M. A. Rowan, M. R. J. Elsegood, *Inorg. Chim. Acta* **2005**, 358, 4067.
- [10] C. K. Z. Andrade, *Curr. Org. Chem.* **2004**, 8, 333.
- [11] K. Mashima, Y. Nakayama, N. Ikushima, M. Kaidzu, A. Nakamura, *J. Organomet. Chem.* **1998**, 566, 111.
- [12] K. Mashima, S. Fujikawa, Y. Tanaka, H. Urata, T. Oshiki, E. Tanaka, A. Nakamura, *Organometallics* **1995**, 14, 2633.
- [13] C. T. Chen, L. H. Doerrer, V. C. Williams, M. L. H. Green, *J. Chem. Soc. Dalton Trans.* **2000**, 967.
- [14] A. Spannenberg, H. Fuhrmann, P. Arndt, W. Baumann, R. Kempe, *Angew. Chem.* **1998**, 110, 3565; *Angew. Chem. Int. Ed.* **1998**, 37, 3363.
- [15] K. Hakala, B. Löfgren, M. Polamo, M. Leskelä, *Macromol. Rapid Commun.* **1997**, 18, 635.
- [16] S. Feng, G. R. Roof, E. Y. X. Chen, *Organometallics* **2002**, 21, 832.
- [17] J. M. Decker, S. J. Geib, T. Y. Meyer, *Organometallics* **1999**, 18, 4417.
- [18] G. Rodriguez, G. C. Bazan, *J. Am. Chem. Soc.* **1995**, 117, 10155.
- [19] a) W. Clegg, M. R. J. Elsegood, S. J. Teat, C. Redshaw, V. C. Gibson, *J. Chem. Soc. Dalton Trans.* **1998**, 3037; b) W. Clegg, *J. Chem. Soc. Dalton Trans.* **2000**, 3223.
- [20] A. Zalkin, D. E. Sands, *Acta Crystallogr.* **1958**, 11, 615.
- [21] L. Higham, M. Thornton-Pett, M. Bochmann, *Polyhedron* **1998**, 17, 3047.
- [22] See for example: a) T. W. Coffindaffer, B. D. Steffy, I. P. Rothwell, K. Foltling, J. C. Huffman, W. E. Streib, *J. Am. Chem. Soc.* **1989**, 111, 4742; b) S. K. Park, S. M. Koo, Y. E. Lee, *Polyhedron* **2000**, 19, 1037.
- [23] G. R. Willey, T. J. Woodman, M. G. B. Drew, *Polyhedron* **1997**, 16, 351.
- [24] A. J. Benton, M. G. B. Drew, R. J. Hobson, D. A. Rice, *J. Chem. Soc. Dalton Trans.* **1981**, 1304.
- [25] H. Kawaguchi, T. Matsuo, *Inorg. Chem.* **2002**, 41, 6090.
- [26] J. M. Hefferis, R. J. Morris, J. C. Huffman, *Inorg. Chem.* **1997**, 36, 3379.
- [27] F. H. Allen, *Acta Crystallogr. Sect. B* **2002**, 58, 380. CSD version 5.27 + 2 updates, May 2006.
- [28] M. Ströbele, H. J. Meyer, *Z. Anorg. Allg. Chem.* **2002**, 628, 488.
- [29] J. A. Canich, F. A. Cotton, S. A. Duraj, *Inorg. Chim. Acta* **1989**, 156, 41.
- [30] V. C. Gibson, T. P. Kee, A. Shaw, *Polyhedron* **1988**, 7, 2217.
- [31] B. Dhawan, C. D. Gutsche, *J. Org. Chem.* **1983**, 48, 1539.
- [32] A. Arduini, A. Casnati in *Macrocyclic Synthesis* (Ed.: D. Parker), Oxford University Press, New York, **1996**, Chapter 7.
- [33] A. L. Spek, *Acta Crystallogr. Sect. A* **1990**, 46, C34.
- [34] a) G. M. Sheldrick, *SHELXTL User Manual* (Version 5), Bruker AXS, Inc., Madison, WI, **1994**; b) SMART, APEX 2, and SAINT software for CCD diffractometers, Bruker AXS, Inc., Madison, WI, **1994**, **2001**, **2003**; c) D. A. Fletcher, R. F. McMeeking, D. Parkin, *J. Chem. Inf. Comput. Sci.* **1996**, 36, 746.
- [35] C. Redshaw, L. Warford, S. H. Dale, M. R. J. Elsegood, *Chem. Commun.* **2004**, 1954.
- [36] H. M. Pritchard, M. Etienne, L. Vendier, G. S. McGrady, *Organometallics* **2004**, 23, 1203.

Received: June 12, 2007
Revised: August 1, 2007
Published online: October 4, 2007